Journal of Biomechanics 166 (2024) 111990

Contents lists available at ScienceDirect

Journal of Biomechanics

journal homepage: www.elsevier.com/locate/jbiomech

The role of the nucleus pulposus in intervertebral disc recovery: Towards improved specifications for nucleus replacement devices

K. Raftery [a,1], T. Rahman [a,b,1], N. Smith [c], T. Schaer [d], N. Newell [a,*]

[a] Department of Bioengineering, Imperial College London, London, UK
[b] Biomechanics Group, Department of Mechanical Engineering, Imperial College London, London, UK
[c] Division of Surgery and Interventional Science, University College London, Stanmore, UK
[d] Department of Clinical Studies New Bolton Center, University of Pennsylvania School of Veterinary Medicine, Kennett Square, PA, USA

ARTICLE INFO

Keywords:
Intervertebral disc
Nuclectomy
Nucleus pulposus
Nucleus Replacement Devices (NRD)
Recovery
Spine

ABSTRACT

Nucleus replacement devices (NRDs) have potential to treat degenerated or herniated intervertebral discs (IVDs). However, IVD height loss is a post-treatment complication. IVD height recovery involves the nucleus pulposus (NP), but the mechanism of this in response to physiological loads is not fully elucidated. This study aimed to characterise the non-linear recovery behaviour of the IVD in intact, post-nuclectomy, and post-NRD treatment states, under physiological loading. 36 bovine IVDs (12 intact, 12 post-nuclectomy, 12 post-treatment) underwent creep-recovery protocols simulating Sitting, Walking or Running, followed by 12 h of recovery. A rheological model decoupled the fluid-independent (elastic, fast) and fluid-dependent (slow) recovery phases. In post-nuclectomy and post-treatment groups, nuclectomy efficiency (ratio of NP removed to remaining NP) was quantified following post-test sectioning. Relative to intact, post-nuclectomy recovery significantly decreased in Sitting (-0.3 ± 0.4 mm, $p < 0.05$) and Walking (-0.6 ± 0.3 mm, $p < 0.001$) coupled with significant decreases to the slow response ($p < 0.05$). Post-nuclectomy, the fast and slow responses negatively correlated with nuclectomy efficiency ($p < 0.05$). In all protocols, the post-treatment group performed significantly worse in recovery (-0.5 ± 0.3 mm, $p < 0.01$) and the slow response ($p < 0.05$). Results suggest the NP mainly facilitates slow-phase recovery, linearly dependent on the amount of NP present. Failure of this NRD to recover is attributed to poor fluid imbibition. Additionally, unconfined NRD performance cannot be extrapolated to the *in vitro* response. This knowledge informs NRD design criteria to provide high osmotic pressure, and encourages testing standards to incorporate long-term recovery protocols.

1. Introduction

Lower back pain (LBP) is estimated to affect 7.5 % of the worldwide population at any given time (Wu et al., 2020), with degenerative disc disease (DDD) majorly contributing to this burden (Zheng and Chen, 2015). DDD likely manifests first in the nucleus pulposus (NP) (Nerlich et al., 1997), a gel-like material within the intervertebral disc (IVD) centre. DDD can also predispose herniation (Urban and Roberts, 2003), for which nuclectomy (or discectomy) is a clinical treatment. Complications arise from both limited (e.g., reherniation (Carragee et al., 2006; Martens et al., 2018)) and aggressive (e.g., disc height loss, collapse, and degeneration (Heo et al., 2017; Rogerson et al., 2019)) discectomy. Nucleus replacement devices (NRDs) aim to reduce these complications by restoring disc height and physiological lumbar spine biomechanics, and thus could offer an intervention for pain arising from early-stage degenerated (i.e., a well-preserved AF) and herniated IVDs (Coric and Mummaneni, 2008).

The IVD is osmoviscoelastic and non-linear in its response to daytime loading and overnight recovery (Reilly et al., 1984). Post-loading, recovery is driven by osmotic pressure exerted by NP proteoglycans (Urban and Maroudas, 1981). Rheological models have previously characterised the recovery response, discretising recovery into the elastic, fast and slow phases.

The slow response is thought to dominate overall recovery, and is dependent on fluid imbibition. The elastic and fast responses are governed by the IVD's intrinsic viscoelasticity (Bezci and O'Connell, 2018)

* Corresponding author at: Department of Bioengineering, Imperial College London, White City Campus, London W12 0BZ, UK
E-mail address: n.newell09@imperial.ac.uk (N. Newell).
[1] Co-first author.

https://doi.org/10.1016/j.jbiomech.2024.111990
Accepted 7 February 2024
Available online 15 February 2024
0021-9290/© 2024 The Author(s). Published by Elsevier Ltd. This is an open access article under the CC BY license (http://creativecommons.org/licenses/by/4.0/).

and is suggested to contribute to 50 % of total disc height restoration (Emanuel et al., 2018). Though NP water uptake is ~ 20 % higher than the AF (Ohshima et al., 1989), it is difficult to discern the role of the NP in both viscoelastic and osmosis-dependent recovery.

Nuclectomy has been shown to decrease the fast-response time constant (τ_1) in creep loading, suggesting that the NP is largely responsible for resisting initial fluid outflow (Johannessen et al., 2006). The effects of nuclectomy on recovery rheological parameters have not been explored. Since the mechanism of recovery is osmotic-dependent, rather than load-dependent (Vergroesen et al., 2016), and the rate of uptake is initially the lowest in the NP (Ohshima et al., 1989), it is plausible to hypothesize the NP is largely responsible for the slow response of recovery.

NRD treatment has been used as an adjunct to aggressive nuclectomy (Ahrens et al., 2009; Balsano et al., 2011; Chen et al., 2023). During NRD testing, it is recommended to incorporate physiological loads to extrapolate *in vivo* performance (ASTM International., 2020). Yet *in vitro* studies rarely use loading regimes which simulate everyday dynamic activities. Furthermore, ASTM standards do not list recovery as a paramount protocol. Thus, the analysis of recovery behaviour has been somewhat omitted in previous studies which aimed to characterise NRDs (e.g., only reporting the restoration of material properties (Bertagnoli et al., 2005; Li et al., 2014), or disc height at a singular timepoint (Thomas et al., 2010; Wilke et al., 2001)). More concerningly, it is common for NRDs to have poor clinical outcomes, and often associated with disc height loss over time (e.g., 18 % lower disc height for PDN (Raymedica, Minneapolis, MN) (Zhang et al., 2009), 11.4 % for NuCore® (SpineWave, Shelton, CT) (Berlemann and Schwarzenbach, 2009)). Further understanding of the role of the NP in recovery may accelerate the development of target properties for new NRD formulations. It is also of interest to understand how unconfined compression testing of NRDs in isolation (in line with ASTM F2346-05) represents the same test *in vitro* (with AF confinement).

The first aim of this study is to compare IVD recovery in intact and post-nuclectomy states, using three physiological loading protocols. The second aim is to assess the ability of NRDs to reinstate intact recovery behaviour, and to associate the standalone biomechanical properties of the NRD in question with its ability to recover the whole IVD.

2. Methods

2.1. Specimen preparation

Fifteen fresh-frozen bovine tails were dissected to remove all soft tissue. The vertebrae were sawn through the mid-transverse plane, yielding 36 functional segment units (FSUs), which were potted in polymethyl-methacrylate (Fig. 1**a**). Fluoroscopy images (InsightFD Mini-C-Arm, Fluoroscan, MA) were taken to ensure the cranial and caudal pots were parallel to the IVD mid-transverse plane. IVD hydration was maintained by regularly spraying with phosphate buffered saline (PBS) at all stages of preparation.

2.1.1. Nuclectomy

The workflow to prepare the intact, post-nuclectomy, and post-treatment groups is outlined in Fig. 1**b**. Post-nuclectomy and post-treatment specimens were subjected to a 20-minute transannular nuclectomy using an automated-shaver (Nucleotome®, Clarus Medical, MN), according to the protocol described by (Rahman et al., 2022). Nuclectomy was considered successful on completion of 20 min of aspiration, as recommended clinically (Arthur et al., 2010; Cannella

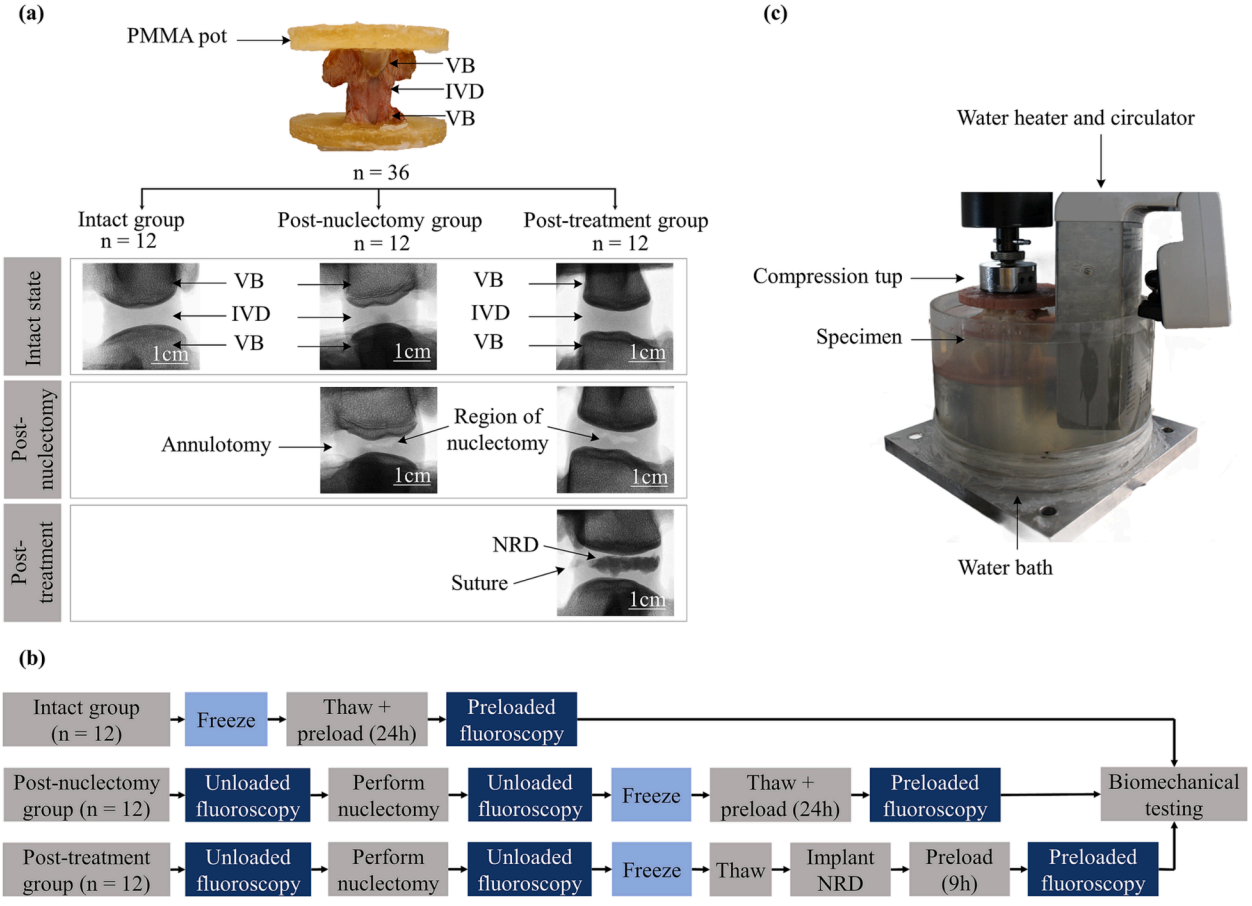


Fig. 1. (a) Schematic of specimen preparation in the intact, post-nuclectomy and post-treatment state. **(b)** Workflow of specimen preparation in intact, post-nuclectomy, and post-treatment conditions. **(c)** Experimental set-up on the screw-driven testing machine with a bovine specimen.

et al., 2014). To measure disc height loss caused by nuclectomy, calibrated fluoroscopy images were taken before and after the procedure in the unloaded state, and disc height was measured using ImageJ (Bethesda, Maryland, USA). Intact and post-nuclectomy specimens were frozen at −20 °C until testing.

2.1.2. NRD treatment

12 thawed nuclectomised specimens underwent NRD treatment immediately prior to testing, since the hydrogel material properties altered upon freezing. An injectable, hydrogel-based, preformed NRD previously developed by Synthes Spine LLP (Philadelphia, USA) was prepared at Imperial College London according to the formulation disclosed in the granted US Patent (US 8,118,874 B2), under the guidance of NS. The NRD was cylindrical in geometry (~2mm in diameter), and was cut into segments ≤ 2 cm in length (volume ≤ 60 mm^3). A syringe was used to inject as many segments as possible through the annulotomy until expulsion occurred. This was closed with two surgical-standard mattress sutures.

2.2. Biomechanical testing

2.2.1. Preload

Intact and nuclectomised specimens were thawed for 24 h in PBS at 4 °C, under 0.06 MPa preload, simulating bedrest (Wilke et al., 1999). This allowed the IVD to reach an equilibrated hydration state. Preliminary work demonstrated ~ 9 h preload was necessary to achieve steady-state displacement (<0.001 mm/s). Due to this, the post-treatment group was preloaded for 9 h at 4 °C.

After preload, fluoroscopy images were taken to measure the preloaded IVD height. Specimens were then placed in a 37 °C PBS bath within a universal testing machine. One additional hour of 0.06 MPa preload allowed the disc to acclimatise to 37 °C. In preliminary tests, insertion of a thermocouple into the NP showed that intradiscal temperature reached 37 °C from 5 °C within 20 min.

2.2.2. Loading & recovery protocol

Intact, post-nuclectomy, and post-treatment groups (N = 12 per group) were sub-grouped to be tested in three loading conditions which simulated typical daytime activities (N = 4). These were 1) Sitting, 2) sitting with interspersion of walking breaks (Walking), and 3) Running (Table 1). Stress magnitudes were based upon established human intradiscal pressures in the L4–L5 IVD (Wilke et al., 1999), corrected with a factor of 0.66. This accounted for the discrepancy between measured intradiscal pressure, and the applied stress to the whole IVD required to generate this pressure (Dreischarf et al., 2013). To convert stress to compressive force, the cross-sectional area of the IVDs prior to testing were measured. Callipers were used to measure the anteroposterior and mediolateral IVD diameters, repeated three times each to improve accuracy. Circular disc geometry was then assumed (Monaco et al., 2016).

Cyclic frequencies for Walking and Running were based on published reports of preferred stride frequency in gait (Danion et al., 2003; Kay and Warren, 2001; Uematsu et al., 2011) and running velocities between 2.5 and 3.5 m/s (Bailey et al., 2017; Cavagna et al., 1997; de Ruiter et al., 2020), respectively. The Running protocol involved cyclic loading for 40 min, in line with a typical run duration. A screw-driven Instron (model 5866, High Wycombe, UK) (Fig. 1**c**) was used for Sitting and Walking tests. A servo-hydraulic Instron (model 8835) was used for the Running tests, as they required a faster cross-head translation speed. Absolute creep displacement was defined as the total height lost during the loading protocol, measured from the preloaded IVD height.

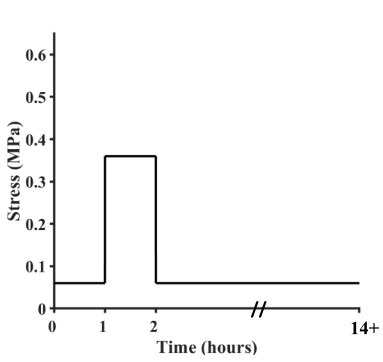
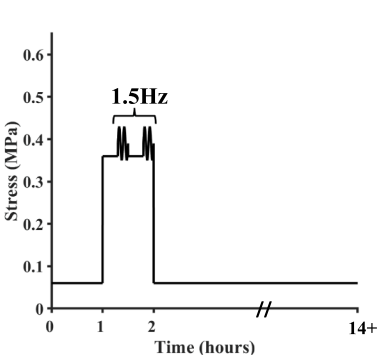
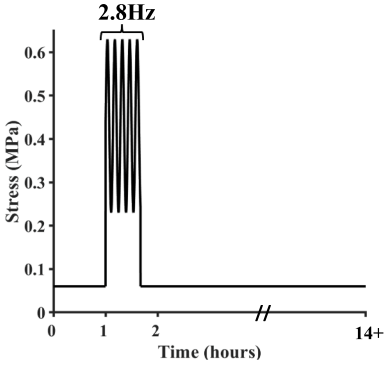
After loading, specimens recovered in the water bath for at least 12 h, with 0.06 MPa applied. Compression ramp rate was 20 N/s and ramp to recovery load was 50 N/s.

2.3. Nuclectomy efficiency and implanted NRD mass

To quantify the amount of NP removed during nuclectomy, the IVDs were sliced transversely after testing, and the remaining NP material was extracted. The aspirated and post-test explants were left to dehydrate via evaporation for 48 h in a fume cupboard before weighing. Nuclectomy efficiency was defined as the ratio between the dry mass of NP removed in the nuclectomy procedure, and the dry mass of the remaining NP material within the IVD.

To quantify the mass of NRD injected, the hydrogel was removed alongside NP removal, and the wet mass was blotted and weighed.

Table 1
Loading durations, magnitudes, and cyclic frequencies for each protocol.

Groups	Sitting			Walking			Running		
	Intact (n = 4)	Post-nuclectomy (n = 4)	Post-treatment (n = 4)	Intact (n = 4)	Post-nuclectomy (n = 4)	Post-treatment (n = 4)	Intact (n = 4)	Post-nuclectomy (n = 4)	Post-treatment (n = 4)
Preload	0.06 MPa, overnight at 4°C and 1 h at 37°C								
Protocol	0.36 MPa, 1 h			0.36 MPa, 2 × 20 min; 960 cycles, 0.35–0.42 MPa, 1.6 Hz, 2 × 10 minutes			6720 cycles, 0.23–0.63 MPa, 2.8 Hz, 40 min		
Recovery	0.06 MPa, 12–14 h								
Stress–time history									

2.4. NRD biomechanical characterisation

Five NRD bores (14 mm diameter, 8 mm height) were submerged in 37 °C PBS, and after a 30-minute equilibration period, were subjected to 25 % compressive strain in increments of 5 %, interspersed with 5 min of stress-relaxation (Cloyd et al., 2007). The toe and linear region moduli were calculated as the tangent to the experimental stress–strain curve at 0 % and 20 % strain, respectively. To characterise swelling capacity, three NRD segments (2 mm diameter, 10 mm length) were dehydrated and immersed in PBS, both for 48 h. At 1, 3, 24, and 48 h, the segments were blotted and weighed.

2.5. Data analysis

2.5.1. Curve fitting

Experimental data was analysed using a custom-written MATLAB code (Mathworks Inc., Natick, MA). The recovery displacement (x_r, mm) as a function of time (t, hours) was fit to a rheological model previously used in creep-recovery analyses of human and bovine IVDs (Bezci et al., 2020a; Bezci and O'Connell, 2018; Keller et al., 1987; O'Connell et al., 2011), using the method of least-squares. The model consists of two Kelvin-Voigt elements and a spring in series:

$$x_r(t) = x_E + A_1(1 - e^{-t/\tau_1}) + A_2(1 - e^{-t/\tau_2}) \quad (1)$$

Where A_1 and A_2 denote the fast and slow displacement constants (mm), τ_1 and τ_2 the fast and slow time constants (hours), and x_E the elastic displacement (mm). The Instron's displacement transducer measured x_E, which was input into the model. Curve fit was evaluated with R^2. Equilibrium time was defined as 99 % of the exponential curve limit. To account for variation in disc height and creep deformation between specimens, x_r at 12 h, x_E, A_1, and A_2 were normalised to the absolute creep displacement for each specimen.

2.5.2. Creation of the fast and slow response indexes

Changes to the A and τ values, attributed to altered loading and IVD morphology, respectively (Vresilovic et al., 2006), were not expected to be independent of one another. As such, analysis of curve profiles based on comparing A and τ separately was complex (although reported for completeness as a supplementary figure (**Figure S1**)). To counter this, an index was created whereby the A and τ parameters were weighted respective to the magnitude to which they affected the recovery curve (e.g., a large change in a τ parameter (or A parameter) may not elicit an equal or linear change to the curve profile and resulting height restoration). These indexes were termed the fast response (a function of A_1 and τ_1) and the slow response (a function of A_2 and τ_2).

To create the fast and slow response values with weighted A and τ parameters, equations were constructed describing the relationship between a change in parameter (A_1, A_2, τ_1, and τ_2, for a given range) *versus* a change in recovery (% IVD height increase) (**Figure S2**). The bounds used for each parameter were based on the experimental data range (A_1 = 2 – 20 %, A_2 = 25 – 105 %, τ_1 = 2 – 30 min, τ_2 = 2 – 12 h). When finding the constants for these equations, one parameter was changed at a time to isolate its effect. The values for the unchanged parameters were arbitrary, calculated as an average across all groups (N = 36).

To quantify the dependency of each parameter on the instantaneous recovery change, timepoints of six minutes (for the fast response) and 12 h (for the slow response) were chosen, as changes to τ at these timepoints elicited a local maximum of recovery change, and are within the period that each response is thought to occur (Bezci and O'Connell, 2018; Masuoka et al., 2007). Using the calculated linear and exponential constants shown as equations in **Figure S2**, the fast and slow responses were described as essentially A: τ ratios:

$$Fast\ response\ index = \frac{0.18(A_1)}{26.6(\tau_1{}^{|-0.11|})} \quad (2)$$

$$Slow\ response\ index = \frac{0.70(A_2)}{|-2.69|(\tau_2)} \quad (3)$$

Where a greater response index represents greater recovery. To ensure all response outcomes were positive, the absolute values of the linear and exponential τ constants were used. The experimental A and τ values were then inputted into these equations to generate a single value to be compared across loading protocols and IVD states.

2.6. Statistical analysis

All statistical analyses were performed in GraphPad Prism (v9.4.1, San Diego, California, USA) with $p = 0.05$. Shapiro-Wilk tests assessed normality. Differences between protocol (Sitting, Walking, Running) and state (intact, post-nuclectomy, post-treatment) were tested with two-way analysis of variance (ANOVA) and Tukey's post-hoc. Linear regression with Pearson's coefficient assessed correlations between recovery parameters and nuclectomy efficiency. Two-way ANOVA was additionally used to compare NRD recovery within the IVD and in isolation with unconfined compression.

3. Results

No significant differences in IVD CSA, height at preload, or height post-loading were found when assessing any interaction between treatment groups and loading conditions (Table 2) ($p > 0.39$). These parameters additionally did not correlate with recovery at 12 h ($p = 0.33$). IVD height decreased 14.8 ± 4.5 % due to nuclectomy. There was no significant difference in nuclectomy efficiency between groups ($p > 0.083$).

3.1. Overall recovery

In all cases, creep displacement rate was negligible after one hour of preload at 37 °C (<0.0001 mm/s). This represented steady-state hydration to which 12-hour height recovery could be normalised to (Fig. 2). The rheological model fit well to the intact and post-nuclectomy data ($R^2 = 0.99 \pm 0.01$), with marginally weaker agreement for the NRD data ($R^2 = 0.94 \pm 0.05$).

All groups recovered non-linearly (Fig. 3). Intact IVD recovery at 12 h did not differ between protocols (mean: 1.3 ± 0.2 mm, $p > 0.44$). Relative to intact, post-nuclectomy recovery significantly decreased in Sitting (-0.3 ± 0.4 mm, $p < 0.05$) and Walking (-0.6 ± 0.3 mm, $p < 0.001$). No differences were observed in Running ($p = 0.74$). Relative to Walking, post-nuclectomy, recovery was significantly increased in Sitting (+0.4 ± 0.3 mm, $p < 0.01$) and Running (+0.5 ± 0.1 mm, $p < 0.0001$). Post–treatment, recovery significantly decreased relative to intact in all protocols (-0.5 ± 0.3 mm, $p < 0.01$), and relative to post-nuclectomy in Sitting and Running only (-0.2 ± 0.3 mm and −0.4 ± 0.2 mm respectively, $p < 0.01$) (Fig. 4**a**).

3.2. Phases of recovery

The elastic and fast responses were not significantly altered in post-nuclectomy and post-treatment groups, relative to intact ($p > 0.12$) (Fig. 4**b,c**). There was no correlation between either responses with recovery at 12 h (Fig. 5**a,b**) ($p > 0.44$). However, relative to intact, the slow response was significantly lower post-nuclectomy in Sitting and Walking ($p < 0.05$), and in all groups post-treatment ($p < 0.05$) (Fig. 4**d**). The slow response and recovery at 12 h were significantly associated ($p < 0.0001$, $R^2 = 0.71$, $r = 0.84$) (Fig. 5**c**).

3.3. Nuclectomy efficiency

Post-nuclectomy specimens displayed a moderate negative

Table 2
Mean (SD) IVD characteristics for each state and loading protocol. Note that preloaded IVD height was measured after performing nuclectomy and / or NRD treatment, under a 0.06 MPa preload. Absolute creep displacement was defined as the total height lost during the loading protocol, measured from the preloaded IVD height. IVD height post-loading was defined as the height immediately prior to recovery. Nuclectomy efficiency was defined as the ratio between the dry mass of NP removed in the nuclectomy procedure, and the dry mass of the remaining NP material within the IVD. * denotes significance between post-nuclectomy and both intact and post-treatment groups, pooled for all loading protocols ($p < 0.05$).

Groups	Sitting			Walking			Running		
	Intact (n=4)	Post-nuclectomy (n=4)	Post-treatment (n=4)	Intact (n=4)	Post-nuclectomy (n=4)	Post-treatment (n=4)	Intact (n=4)	Post-nuclectomy (n=4)	Post-treatment (n=4)
Preloaded IVD height (mm)	9.4 (0.7)	9.2 (0.6)	10.7 (0.6)	8.7 (2.3)	9.5 (1.5)	8.4 (3.1)	10.3 (2.0)	9.8 (1.8)	9.6 (1.3)
IVD creep displacement (mm)	1.40 (0.26)	1.35* (0.22)	1.51 (0.11)	1.53 (0.24)	1.25* (0.16)	1.51 (0.12)	1.54 (0.20)	1.28* (0.06)	1.48 (0.13)
IVD height post-loading (mm)	6.9 (1.0)	6.9 (0.7)	8.0 (1.1)	6.3 (2.0)	7.2 (1.3)	7.4 (1.4)	8.3 (1.8)	8.3 (1.7)	7.3 (1.2)
IVD CSA (mm^2)	480.8 (61.9)	502.6 (25.0)	525.8 (53.6)	472.9 (47.3)	513.5 (45.3)	463.8 (47.4)	460.6 (70.8)	537.1 (44.0)	517.3 (63.0)
Nuclectomy efficiency (%)	–	47.3 (18.7)	62.3 (13.6)	–	75.2 (8.4)	37.3 (11.0)	–	60.2 (13.2)	73.7 (27.3)

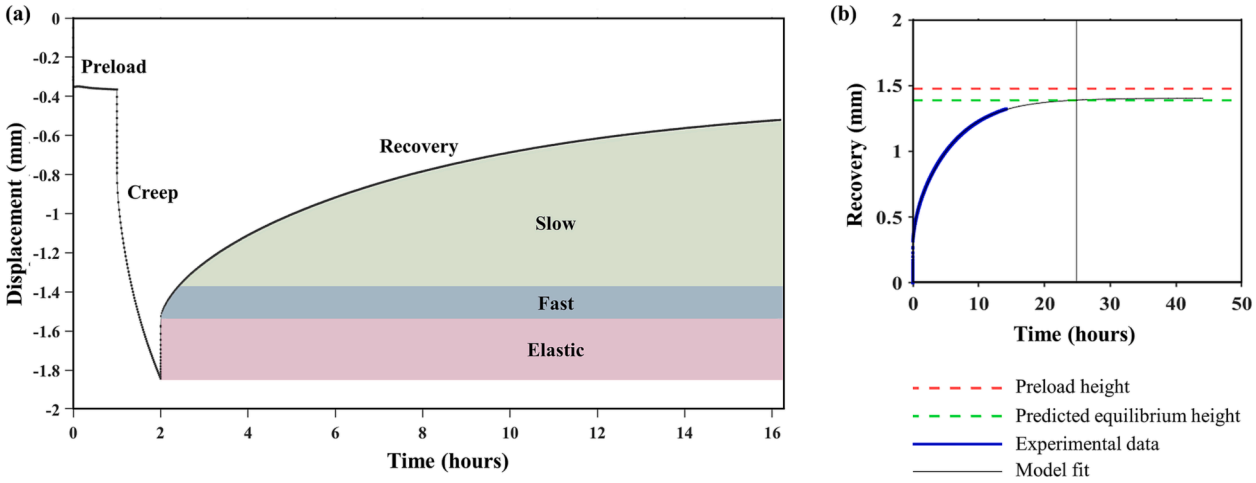


Fig. 2. (a) Experimental creep-recovery data (Sitting protocol) from one specimen acquired on the screw-driven testing machine. Disc was preloaded ($0 < t < 1$), creep loaded ($1 < t < 2$) and allowed to recover ($t > 2$). 0 mm represents displacement at initial contact with the actuator. Pink, blue, and green regions denote approximations of the elastic, fast, and slow responses, with respect to the rheological model. **(b)** Recovery was normalised to the height at preload (red dashed line). The experimental data (blue dots) were fit to the viscoelastic model (black line), which predicted the equilibrium height (green dashed line) and time (black vertical line). (For interpretation of the references to colour in this figure legend, the reader is referred to the web version of this article.)

correlation between nuclectomy efficiency and recovery at 12 h ($R^2 = 0.38$, $p < 0.05$, r = -0.62) (Fig. 6**a**). Additionally, nuclectomy efficiency negatively correlated with both the fast and slow response ($R^2 > 0.46$, $p < 0.05$, r = -0.70) (Fig. 6**c,d**).

In the post-treatment groups, the recovery parameters were independent of nuclectomy efficiency (Fig. 6**a-d**). The mass of NRD injected (on average 108.95 ± 49.10 mg) strongly correlated with the slow response, correcting for disc CSA ($R^2 = 0.57$, r = 0.76, $p < 0.05$). Following sectioning, it was observed that the NRD often did not fill the NP cavity (Fig. 6**e**).

3.4. NRD characterisation

The NRD exhibited a toe and linear modulus of 23.6 ± 2.7 kPa and 144.0 ± 14.6 kPa, respectively (Fig. S3**a**). Maximum mass fold change was 3.0 ± 0.08 and was reached by 24 h of free swelling (Fig. S3**b**).

4. Discussion

It is important to delineate the recovery behaviour of the NP under different physiological scenarios to mimic these properties when developing NRD formulations. In this study, the elastic and osmo-viscoelastic phases of recovery were investigated by combining the time and displacement constants. In creep, Vresilovic *et al.* used a biexponential model to suggest that the time constant dictates the fluid flow mechanism, altered by nuclectomy, whilst the displacement constant represents the fluid volume, altered by the load (Vresilovic et al., 2006). Though a five-parameter model was used in this study, it supports the finding that both the A and τ values were altered by treatment and loading type (**Figure S1**). Thus, conclusions regarding rheological behaviour in future studies investigating both morphological status and loading type may be better drawn by considering both parameters of each response together.

Intact IVDs recovered consistently and irrespective of loading stress or dynamic frequency (Fig. 4**a**). Independence of τ_1 and τ_2 to creep load has been demonstrated (Bezci et al., 2020a), and non-linear recovery after static and dynamic loading has been reported as superimposable (van der Veen et al., 2007). However, post-nuclectomy recovery at 12 h was significantly lower than intact in Sitting and Walking, and recovery across all groups strongly correlated with the slow response (Fig. 5**c**). Solution osmolarity has previously been shown to affect the magnitude of the slow response, but not the fast (Bezci and O'Connell, 2018).

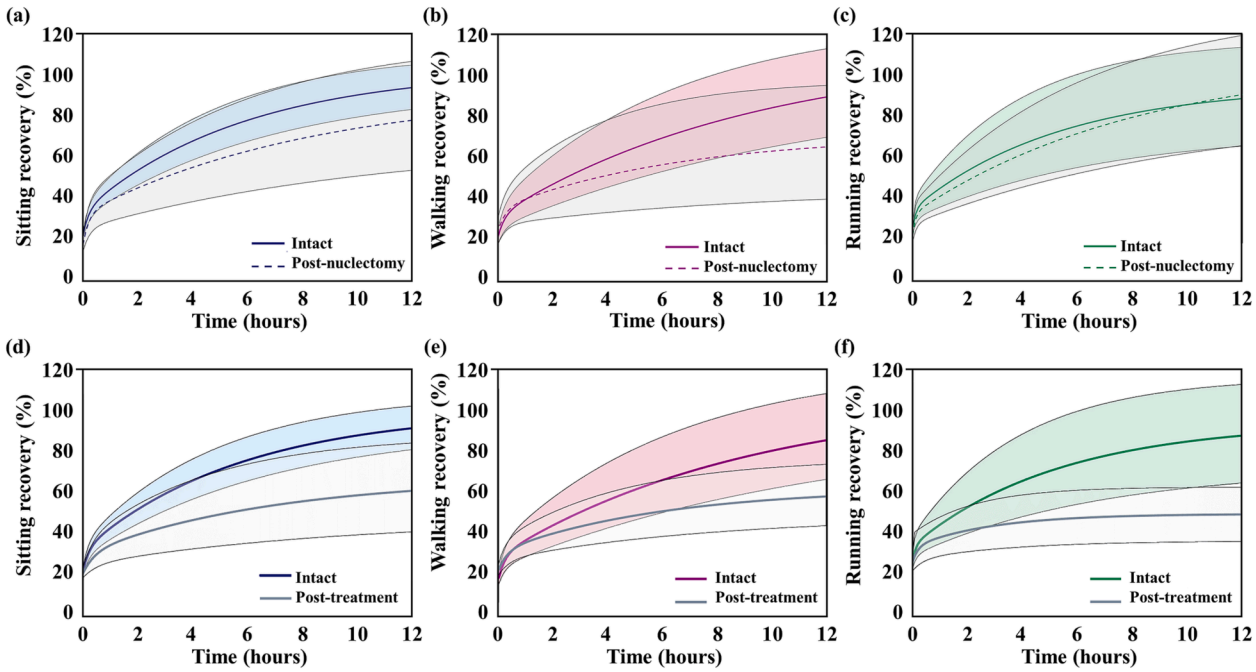


Fig. 3. Mean (SD) recovery-time plots for **(a-c)** intact, post-nuclectomy and **(d-f)** post-treatment specimens in the **(a,d)** Sitting, **(b,e)** Walking and **(c,f)** Running protocols.

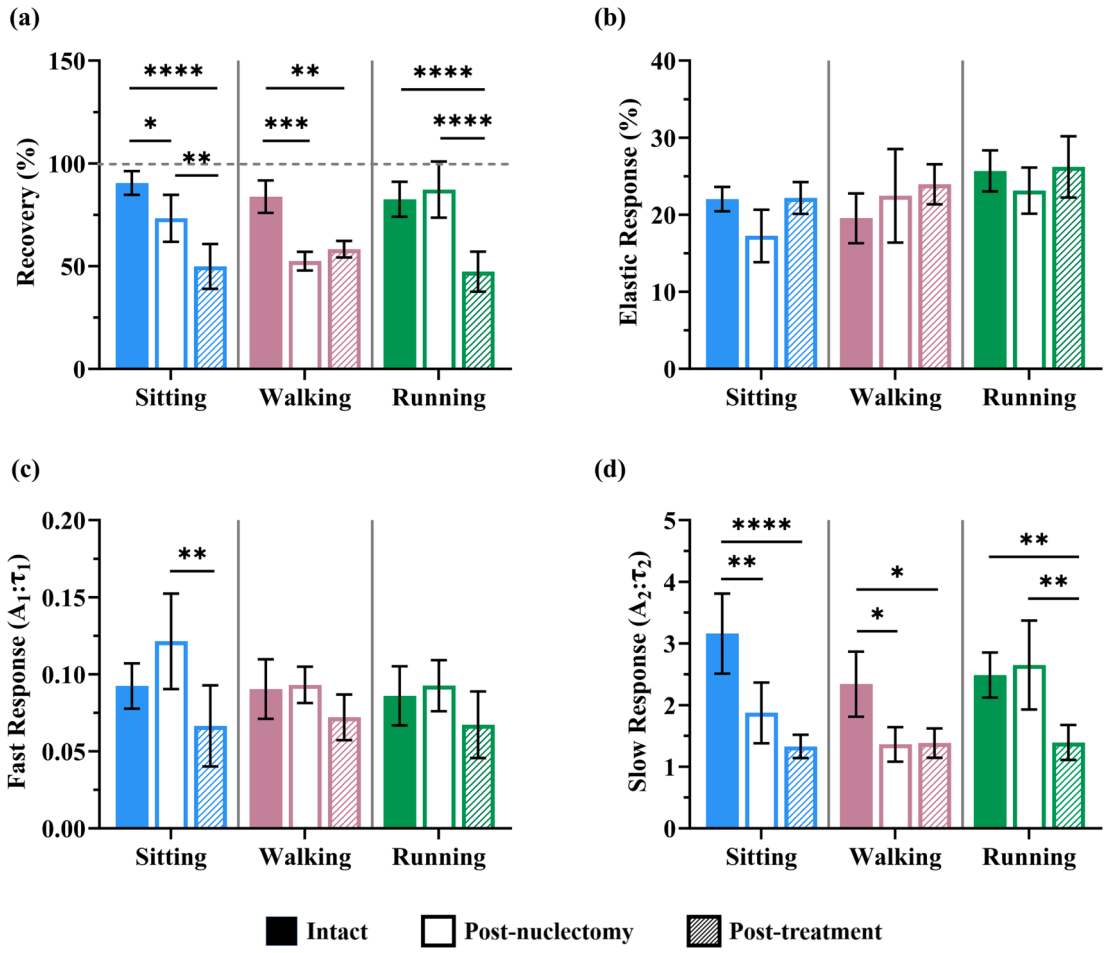


Fig. 4. **(a)** Overall recovery at 12 h, **(b)** elastic response, **(c)** fast response and **(d)** slow response. 100 % recovery (dashed line) indicates a complete restoration of the height prior to loading. * $p < 0.05$, *** $p < 0.001$, **** $p < 0.0001$.

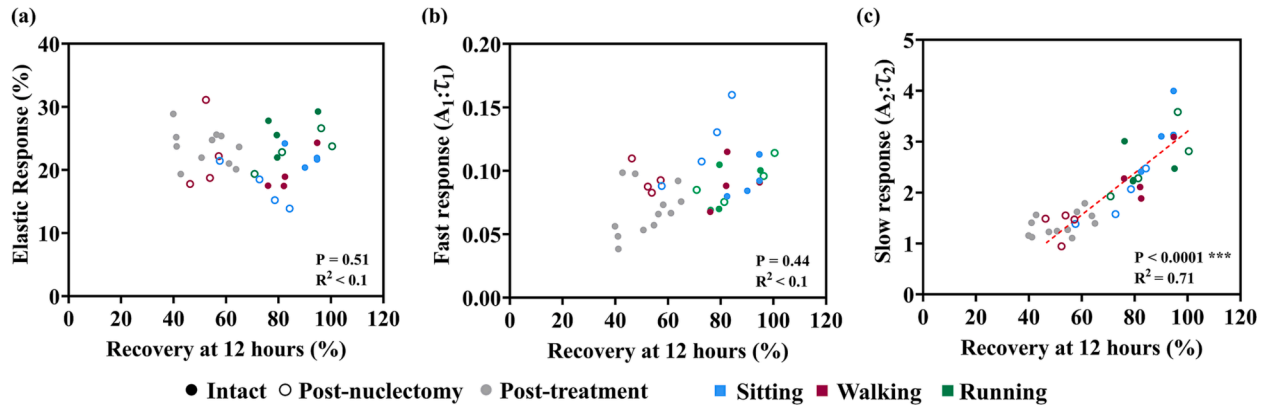


Fig. 5. Relationship between overall recovery at 12 h and the **(a)** elastic, **(b)** fast and **(c)** slow response. Red dashed line = regression fit where significance was found. Note that data from the NRD-treated group (grey) was not included in the regression analysis but is presented for reference. (For interpretation of the references to colour in this figure legend, the reader is referred to the web version of this article.)

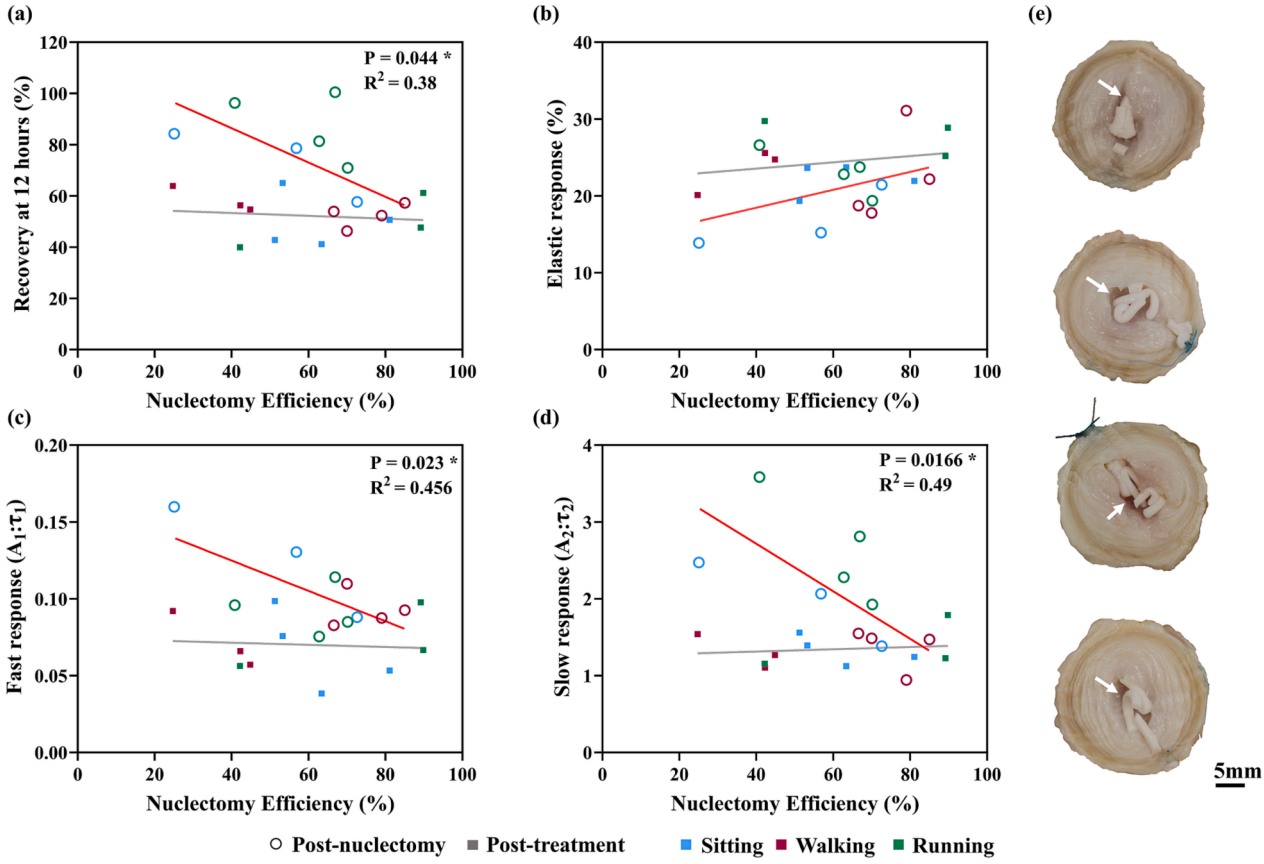


Fig. 6. Relationship between the nuclectomy efficiency and **(a)** overall recovery at 12 h, **(b)** elastic, **(c)** fast and **(d)** slow response. Red dashed line = regression fit where significance was found. Note that data from the NRD-treated group (grey line) was not included in the regression analysis but is presented for reference. **(e)** Axial view of four typical bovine IVDs cut transversely post-test. The white arrows point to the NRD material filling the NP cavity. (For interpretation of the references to colour in this figure legend, the reader is referred to the web version of this article.)

Additionally, NP internal pressure has been reported to increase by ~ 300 kPa after a 700 kPa decrease in environmental osmotic pressure (molar concentration * gas constant * temperature) (Emanuel et al., 2018). Taken together, it is deduced that NP-driven fluid imbibition is required for full height restoration, whereas the elastic and fast responses mainly operate through AF viscoelastic recoil.

Running exhibited comparable overall recovery and slow responses between intact and post-nuclectomy groups (Fig. 5**a**). This could suggest reliance on NP-driven recovery after loads of low magnitude and frequency (<2Hz). Exceeding this loading rate and magnitude, the AF may absorb more energy than the NP (Cannella et al., 2008; Newell et al., 2019). Additionally, high frequency loading may encourage the remaining NP to redistribute within the cavity. Without physical endplate boundaries, the NP volume expands to be considerably larger than the NP cavity (Bezci et al., 2020b). Thus, it is possible that the remaining NP repressurised the IVD and improved recovery behaviour, as has been observed previously (Claeson et al., 2019; Johannessen et al., 2006), though restoration to the pre-nuclectomy height is unlikely.

However, it is plausible that nuclectomy efficiency confounded this result. Though not significant, more NP material was removed in the Walking group relative to Running. In fact, over intact and post-nuclectomy groups, overall recovery and the slow response were linearly dependent on nuclectomy efficiency (Fig. 6**a,d**). The effects of limited *versus* aggressive nuclectomy have been observed for other biomechanical (increased range of motion) and non-linear (decreased viscous damping) properties (Johannessen et al., 2006). Similar trends in this study are likely due to the loss of proteoglycans proportional to NP removal. Further efforts should focus on quantifying a nuclectomy threshold whereby IVD recovery is excessively compromised, it may provide surgeons with a limit when performing aggressive discectomy.

The fast response also correlated with nuclectomy efficiency (Fig. 6**c**). This may be a by-product of the "synergistic" interaction between the NP and AF (Joshi et al., 2003). Without NP pressurisation, the AF is susceptible to inwards bulging and shear (Hwang et al., 2012), associated with predisposition to injury (Goel et al., 1995). Thus, declining AF integrity may be represented by a reduced fast response.

Post-treatment recovery was significantly lower than intact (Fig. 4**a**), coupled with a significant decrease in the slow response (Fig. 4**d**). The NRD used in this study was 10x stiffer than previously characterised human NP (Cloyd et al., 2007). Furthermore, whilst the NRD swelling capacity (3 ± 0.08x) was comparable to previously-characterised bovine NP explants (3x at 0.15 M (Bezci et al., 2020b), this NRD was fully hydrated, whilst the explants were not. This suggests native NP has more residual capacity to swell and exert hoop stresses on the AF. It is therefore expected that without confinement from the AF, the isolated NRD would not behave in a similar manner to the NRD-treated IVD. Indeed, supplementary data from NRD bores in unconfined compression demonstrated that there was a marked change to both the recovery-time profile (Fig. S4**a-c**) and the proportion of elastic recovery relative to the time-dependent phases (Fig. S4**d,e**), when subjected to the same loading protocols. Taken together, NRD formulation should above all focus on the ability of the material to uptake fluid.

Further impediment to recovery may have arisen from the NRD preventing the redistribution of remaining NP. This was inferred from the post-treatment recovery parameters being independent of nuclectomy efficiency (Fig. 6). Acknowledging that this model does not fully represent the behaviour of degenerated human IVDs, results suggest there is no NP removal threshold when performing discectomy prior to NRD treatment, reducing the concerns of aggressive discectomy.

This study bears some limitations. Human FSUs would account for degeneration and facet load-bearing, concomitant with disc height loss (Adams et al., 2006). However, bovine IVDs bear similar proteoglycan content relative to non-degenerate human (Beckstein et al., 2008), and control variability arising from degeneration, sex, age, and spinal level (Urban and Roberts, 2003). It is also worth noting that given the time to equilibrium (~9 h in this study) is longer than what would be expected for *in vivo* recovery, the hydration state of the samples may not replicate physiological creep-recovery dynamics. It is theorised that *in vivo,* creep time constants are up to 5x shorter than recovery, enabling the IVD to maintain its height in a "steady-state" without the requirement of reaching equilibrium (O'Connell et al., 2011; Vergroesen et al., 2016).

The procedure of annulotomy and AF closure may in part explain poor recovery in post-nuclectomy and post-treatment groups. Annular injury is suspected to decrease fluid flow resistance into the NP, proportional to the size of the defect (Michalek and Iatridis, 2011), and the amount of NP proteoglycan. This may explain why the fast response was not significantly altered by nuclectomy, but negatively correlated with nuclectomy efficiency (Fig. 6**c**). However, preliminary data did not indicate annulotomy, nor an AF suture, would alter short-term recovery (**Figure S5**).

Both annulotomy and nuclectomy have been previously shown to reduce IVD compressive stiffness (Michalek et al., 2010; Rahman et al., 2022). However, this is potentially independent to recovery performance, as puncture models exhibit similar hysteresis (Michalek and Iatridis, 2012) and increased recovery displacement (Reitmaier et al., 2012) relative to intact. In the present study, absolute recovery displacement remained the lowest in the post-treatment group, whilst after loading, IVD height was comparable among groups, demonstrating that recovery was not confounded by compressive stiffness.

Lastly, implantation of preformed NRD may have attenuated interactions with the inner AF. If the cavity is unfilled, FSU stiffness (Joshi et al., 2005; Reitmaier et al., 2012), range of motion, and intradiscal pressure (Arthur et al., 2010; Cannella et al., 2014) are compromised. Whilst the suture itself may not influence IVD creep-recovery, it is an insufficient method to retain the volume of NRD which would restore intradiscal pressure (Reitmaier et al., 2012) (Fig. 6**e**). This would explain why the post-treatment slow response significantly correlated with the mass of NRD inserted ($r = 0.76$, $p < 0.05$). Use of materials cured *in situ*, combined with more robust AF closure devices, are recommended in future investigations of recovery.

5. Conclusions

This study enhances clarity on the ideal properties of an artificial nucleus and the regimens required for *in vitro* testing. The NP drives the osmotic-dependent (slow) recovery response, where the amount of NP removed appears to be more important than the loading protocol. Surprisingly, NRD treatment was unable to restore intact and even post-nuclectomy recovery behaviour, suggesting an inability to recreate NP osmotic pressure due to the NRD properties and the insufficient volume of NRD implanted, subject to the AF closure method. Based on these findings, recovery testing should 1) be a paramount procedure, 2) be conducted for at least 12 h, and 3) consider the interaction between remaining native NP, inner AF, and NRD. These recommendations could contribute to the clinical success of future NRDs by ensuring the long-term restoration of disc height *in vivo*.

Author contribution

KR, TR and NN designed the study. KR and TR collected the experimental data. KR drafted the manuscript and analysed the data. The manuscript was edited by all authors. TS supplied the automated shaver for nuclectomy. NS supplied the formulation and materials in which to synthesise the NRD.

CRediT authorship contribution statement

K. Raftery: Writing – review & editing, Writing – original draft, Visualization, Project administration, Methodology, Investigation, Formal analysis, Data curation, Conceptualization. **T. Rahman:** Writing – review & editing, Writing – original draft, Supervision, Project administration, Methodology, Investigation, Funding acquisition, Data curation, Conceptualization. **N. Smith:** Writing – review & editing, Resources, Conceptualization. **T. Schaer:** Writing – review & editing, Resources, Conceptualization. **N. Newell:** Writing – review & editing, Supervision, Resources, Project administration, Methodology, Funding acquisition, Conceptualization.

Declaration of competing interest

The authors declare the following financial interests/personal relationships which may be considered as potential competing interests: NS was involved in the development and patenting of hydrogel-based technologies for Synthes Spine as Director of Non Fusion Technologies.

Acknowledgements

The authors gratefully acknowledge Watson Medical Ltd for partially funding the EPSRC DTP CASE Conversion Studentship for TR (EP/R513052/1).

Appendix A. Supplementary data

Supplementary data to this article can be found online at https://doi.org/10.1016/j.jbiomech.2024.111990.

References

Adams, M.A., Pollintine, P., Tobias, J.H., Wakley, G.K., Dolan, P., 2006. Intervertebral disc degeneration can predispose to anterior vertebral fractures in the thoracolumbar spine. J. Bone. Miner. Res. 21 https://doi.org/10.1359/jbmr.060609.

Ahrens, M., Tsantrizos, A., Donkersloot, P., Martens, F., Lauweryns, P., le Huec, J.C., Moszko, S., Fekete, Z., Sherman, J., Yuan, H.A., Halm, H., 2009. Nucleus Replacement With the DASCOR Disc Arthroplasty Device. Spine (Phila Pa 1976) 34. 10.1097/brs.0b013e3181a3967f.

Arthur, A., Cannella, M., Keane, M., Singhatat, W., Vresilovic, E., Marcolongo, M., 2010. Fill of the nucleus cavity affects mechanical stability in compression, bending, and torsion of a spine segment, which has undergone nucleus replacement. Spine (Phila Pa 1976) 35. 10.1097/BRS.0b013e3181bdbb1a.

ASTM International., 2020. F2346-18: Standard Test Methods for Static and Dynamic Characterisation of Spinal Artificial Discs. 12:15:18 EDT.

Bailey, J., Mata, T., Mercer, J., 2017. Is the Relationship Between Stride Length, Frequency, and Velocity Influenced by Running on a Treadmill or Overground? Int. J. Exerc. Sci. 10, 1067–1075.

Balsano, M., Zachos, A., Ruggiu, A., Barca, F., Tranquilli-Leali, P., Doria, C., 2011. Nucleus disc arthroplasty with the NUBAC^{TM} device: 2-year clinical experience. Eur. Spine. J. 20, 36–40. https://doi.org/10.1007/s00586-011-1752-3.

Beckstein, J.C., Sen, S., Schaer, T.P., Vresilovic, E.J., Elliott, D.M., 2008. Comparison of animal discs used in disc research to human lumbar disc: Axial compression mechanics and glycosaminoglycan content. Spine (Phila Pa 1976) 33. 10.1097/BRS.0b013e318166e001.

Berlemann, U., Schwarzenbach, A.O., 2009. An injectable nucleus replacement as an adjunct to microdiscectomy: 2 year follow-up in a pilot clinical study. Eur. Spine. J. 18, 1706–1712. https://doi.org/10.1007/s00586-009-1136-0.

Bertagnoli, R., Sabatino, C.T., Edwards, J.T., Gontarz, G.A., Prewett, A., Parsons, J.R., 2005. Mechanical testing of a novel hydrogel nucleus replacement implant. Spine. J. https://doi.org/10.1016/j.spinee.2004.12.004.

Bezci, S.E., O'Connell, G.D., 2018. Osmotic Pressure Alters Time-dependent Recovery Behavior of the Intervertebral Disc. Spine (Phila Pa 1976) 43. 10.1097/BRS.0000000000002354.

Bezci, S.E., Lim, S., O'Connell, G.D., 2020a. Nonlinear stress-dependent recovery behavior of the intervertebral disc. J. Mech. Behav. Biomed. Mater 110. https://doi.org/10.1016/j.jmbbm.2020.103881.

Bezci, S.E., Torres, K., Carraro, C., Chiavacci, D., Werbner, B., Lim, S., O'Connell, G.D., 2020b. Transient swelling behavior of the bovine caudal disc. J. Mech. Behav. Biomed. Mater 112. https://doi.org/10.1016/j.jmbbm.2020.104089.

Cannella, M., Arthur, A., Allen, S., Keane, M., Joshi, A., Vresilovic, E., Marcolongo, M., 2008. The role of the nucleus pulposus in neutral zone human lumbar intervertebral disc mechanics. J. Biomech 41. https://doi.org/10.1016/j.jbiomech.2008.04.037.

Cannella, M., Isaacs, J.L., Allen, S., Orana, A., Vresilovic, E., Marcolongo, M., 2014. Nucleus implantation: The biomechanics of augmentation versus replacement with varying degrees of nucleotomy. J. Biomech. Eng 136. https://doi.org/10.1115/1.4027056.

Carragee, E.J., Spinnickie, A.O., Alamin, T.F., Paragioudakis, S., 2006. A prospective controlled study of limited Versus subtotal posterior discectomy: Short-term outcomes in patients with herniated lumbar intervertebral discs and large posterior anular defect. Spine (Phila Pa 1976) 31. 10.1097/01.brs.0000203714.76250.68.

Cavagna, G.A., Mantovani, M., Willems, P.A., Musch, G., 1997. The resonant step frequency in human running. Pflugers. Arch 434. https://doi.org/10.1007/s004240050451.

Chen, X., Kohan, S., Bhargav, D., Choi, J., Perera, S., Dean, C., Chopra, N., Sial, A., Sandhu, H.S., Apos, E., Appleyard, R., Diwan, A.D., 2023. Phase 1 evaluation of an elastomeric nucleus pulposus device as an option to augment disc at microdiscectomy: Experimental results from biomechanical and biocompatibility testing and first in human. JOR. Spine. https://doi.org/10.1002/jsp2.1250.

Claeson, A.A., Vresilovic, E.J., Showalter, B.L., Wright, A.C., Gee, J.C., Malhotra, N.R., Elliott, D.M., 2019. Human disc nucleotomy alters annulus fibrosus mechanics at both reference and compressed loads. J. Biomech. Eng 141. https://doi.org/10.1115/1.4043874.

Cloyd, J.M., Malhotra, N.R., Weng, L., Chen, W., Mauck, R.L., Elliott, D.M., 2007. Material properties in unconfined compression of human nucleus pulposus, injectable hyaluronic acid-based hydrogels and tissue engineering scaffolds. Eur. Spine. J. 16 https://doi.org/10.1007/s00586-007-0443-6.

Coric, D., Mummaneni, P.V., 2008. Nucleus replacement technologies. J. Neurosurg. Spine 8. https://doi.org/10.3171/spi/2008/8/2/115.

Danion, F., Varraine, E., Bonnard, M., Pailhous, J., 2003. Stride variability in human gait: The effect of stride frequency and stride length. Gait. Posture 18. https://doi.org/10.1016/S0966-6362(03)00030-4.

de Ruiter, C.J., van Daal, S., van Dieën, J.H., 2020. Individual optimal step frequency during outdoor running. Eur. J. Sport. Sci 20. https://doi.org/10.1080/17461391.2019.1626911.

Dreischarf, M., Rohlmann, A., Zhu, R., Schmidt, H., Zander, T., 2013. Is it possible to estimate the compressive force in the lumbar spine from intradiscal pressure measurements? A finite element evaluation. Med. Eng. Phys 35. https://doi.org/10.1016/j.medengphy.2013.03.007.

Emanuel, K.S., van der Veen, A.J., Rustenburg, C.M.E., Smit, T.H., Kingma, I., 2018. Osmosis and viscoelasticity both contribute to time-dependent behaviour of the intervertebral disc under compressive load: A caprine in vitro study. J. Biomech 70. https://doi.org/10.1016/j.jbiomech.2017.10.010.

Goel, V.K., Wilder, D.G., Pope, M.H., Thomas Edwards, W., 1995. Controversy biomechanical testing of the spine load-controlled versus displacement- controlled analysis. Spine (Phila Pa 1976) 20. 10.1097/00007632-199511000-00017.

Heo, J.H., Kim, C.H., Chung, C.K., Choi, Y., Seo, Y.G., Kim, D.H., Park, S.B., Moon, J.H., Heo, W., Jung, J.M., 2017. Quantity of disc removal and radiological outcomes of percutaneous endoscopic lumbar discectomy. Pain. Physician 20.

Hwang, D., Gabai, A.S., Yu, M., Yew, A.G., Hsieh, A.H., 2012. Role of load history in intervertebral disc mechanics and intradiscal pressure generation. Biomech. Model. Mechanobiol 11. https://doi.org/10.1007/s10237-011-0295-1.

Johannessen, W., Cloyd, J.M., O'Connell, G.D., Vresilovic, E.J., Elliott, D.M., 2006. Trans-endplate nucleotomy increases deformation and creep response in axial loading. Ann. Biomed. Eng 34. https://doi.org/10.1007/s10439-005-9070-8.

Joshi, A., Vresilovic, E., Marcolongo, M., Lowman, A., Karduna, A., 2003. The effect of hydrogel nucleus implant on the mechanical behavior of the lumbar functional spinal unit: An experimental study, in: Proceedings of the IEEE Annual Northeast Bioengineering Conference, NEBEC. 10.1109/nebc.2003.1216068.

Joshi, A., Mehta, S., Vresilovic, E., Karduna, A., Marcolongo, M., 2005. Nucleus implant parameters significantly change the compressive stiffness of the human lumbar intervertebral disc. J. Biomech. Eng 127. https://doi.org/10.1115/1.1894369.

Kay, B.A., Warren, W.H., 2001. Coupling of posture and gait: Mode locking and parametric excitation. Biol. Cybern 85. https://doi.org/10.1007/PL00008002.

Keller, T.S., Spengler, D.M., Hansson, T.H., 1987. Mechanical behavior of the human lumbar spine. I. Creep analysis during static compressive loading. J. Orthopaedic. Res. 5 https://doi.org/10.1002/jor.1100050402.

Li, Z., Kaplan, K.M., Wertzel, A., Peroglio, M., Amit, B., Alini, M., Grad, S., Yayon, A., 2014. Biomimetic fibrin-hyaluronan hydrogels for nucleus pulposus regeneration. Regenerative. Med 9. https://doi.org/10.2217/rme.14.5.

Martens, F., Vajkoczy, P., Jadik, S., Hegewald, A., Stieber, J., Hes, R., 2018. Patients at the Highest Risk for Reherniation Following Lumbar Discectomy in a Multicenter Randomized Controlled Trial. JBJS Open Access 3, e0037.

Masuoka, K., Michalek, A.J., MacLean, J.J., Stokes, I.A.F., Iatridis, J.C., 2007. Different effects of static versus cyclic compressive loading on rat intervertebral disc height and water loss in vitro. Spine (Phila Pa 1976) 32. 10.1097/BRS.0b013e318133d591.

Michalek, A.J., Funabashi, K.L., Iatridis, J.C., 2010. Needle puncture injury of the rat intervertebral disc affects torsional and compressive biomechanics differently. Eur. Spine. J. 19 https://doi.org/10.1007/s00586-010-1473-z.

Michalek, A.J., Iatridis, J.C., 2011. Penetrating annulus fibrosus injuries affect dynamic compressive behaviors of the intervertebral disc via altered fluid flow: An analytical interpretation. J. Biomech. Eng 133. https://doi.org/10.1115/1.4004915.

Michalek, A.J., Iatridis, J.C., 2012. Height and torsional stiffness are most sensitive to annular injury in large animal intervertebral discs. Spine J. 12 https://doi.org/10.1016/j.spinee.2012.04.001.

Monaco, L.A., Dewitte-Orr, S.J., Gregory, D.E., 2016. A comparison between porcine, ovine, and bovine intervertebral disc anatomy and single lamella annulus fibrosus tensile properties. J. Morphol 277. https://doi.org/10.1002/jmor.20492.

Nerlich, A.G., Schleicher, E.D., Boos, N., 1997. Immunohistologic markers for age-related changes of human lumbar intervertebral discs. Spine (Phila Pa 1976) 22. 10.1097/00007632-199712150-00001.

Newell, N., Carpanen, D., Evans, J.H., Pearcy, M.J., Masouros, S.D., 2019. Mechanical Function of the Nucleus Pulposus of the Intervertebral Disc under High Rates of Loading. Spine (Phila Pa 1976) 44. 10.1097/BRS.0000000000003092.

O'Connell, G.D., Jacobs, N.T., Sen, S., Vresilovic, E.J., Elliott, D.M., 2011. Axial creep loading and unloaded recovery of the human intervertebral disc and the effect of degeneration. J. Mech. Behav. Biomed. Mater 4. https://doi.org/10.1016/j.jmbbm.2011.02.002.

Ohshima, H., Tsuji, H., Hirano, N., Ishihara, H., Katoh, Y., Yamada, H., 1989. Water diffusion pathway, swelling pressure, and biomechanical properties of the intervertebral disc during compression load. Spine (Phila Pa 1976) 14. 10.1097/00007632-198911000-00017.

Rahman, T., Baxan, N., Murray, R.T., Tavana, S., Schaer, T.P., Smith, N., Bull, J., Newell, N., 2022. An in vitro comparison of three nucleus pulposus removal techniques for partial intervertebral disc replacement: An ultra-high resolution <scp>MRI</scp> study. JOR. Spine. https://doi.org/10.1002/jsp2.1232.

Reilly, T., Tyrrell, A., Troup, J.D.G., 1984. Circadian variation in human stature. Chronobiol. Int 1. https://doi.org/10.3109/07420528409059129.

Reitmaier, S., Wolfram, U., Ignatius, A., Wilke, H.J., Gloria, A., Martín-Martínez, J.M., Silva-Correia, J., Miguel Oliveira, J., Luís Reis, R., Schmidt, H., 2012. Hydrogels for nucleus replacement-Facing the biomechanical challenge. J. Mech. Behav. Biomed. Mater 14. https://doi.org/10.1016/j.jmbbm.2012.05.010.

Rogerson, A., Aidlen, J., Jenis, L.G., 2019. Persistent radiculopathy after surgical treatment for lumbar disc herniation: causes and treatment options. Int. Orthop 43. https://doi.org/10.1007/s00264-018-4246-7.

Thomas, J.D., Fussell, G., Sarkar, S., Lowman, A.M., Marcolongo, M., 2010. Synthesis and recovery characteristics of branched and grafted PNIPAAm-PEG hydrogels for the development of an injectable load-bearing nucleus pulposus replacement. Acta. Biomater 6. https://doi.org/10.1016/j.actbio.2009.10.024.

Uematsu, A., Inoue, K., Hobara, H., Kobayashi, H., Iwamoto, Y., Hortobágyi, T., Suzuki, S., 2011. Preferred step frequency minimizes veering during natural human walking. Neurosci. Lett 505. https://doi.org/10.1016/j.neulet.2011.10.057.

Urban, J.P.G., Maroudas, A., 1981. Swelling of the intervertebral disc in vitro. Connect. Tissue. Res 9. https://doi.org/10.3109/03008208109160234.

Urban, J., Roberts, S., 2003. Degeneration of the Intervertebral Disc. Arth. Res. &. Ther 5, 120–130.
van der Veen, A.J., van Dieën, J.H., Nadort, A., Stam, B., Smit, T.H., 2007. Intervertebral disc recovery after dynamic or static loading in vitro: Is there a role for the endplate? J. Biomech 40. https://doi.org/10.1016/j.jbiomech.2006.10.018.
Vergroesen, P.P.A., van der Veen, A.J., Emanuel, K.S., van Dieën, J.H., Smit, T.H., 2016. The poro-elastic behaviour of the intervertebral disc: A new perspective on diurnal fluid flow. J. Biomech 49. https://doi.org/10.1016/j.jbiomech.2015.11.041.
Vresilovic, E.J., Johannessen, W., Elliott, D.M., 2006. Disc mechanics with trans-endplate partial nucleotomy are not fully restored following cyclic compressive loading and unloaded recovery. J. Biomech. Eng 128. https://doi.org/10.1115/1.2354210.
Wilke, H.J., Neef, P., Caimi, M., Hoogland, T., Claes, L.E., 1999. New in vivo measurements of pressures in the intervertebral disc in daily life. Spine (Phila Pa 1976) 24. 10.1097/00007632-199904150-00005.
Wilke, H.J., Kavanagh, S., Neller, S., Haid, C., Claes, L.E., 2001. Effect of a prosthetic disc nucleus on the mobility and disc height of the L4–5 intervertebral disc postnucleotomy. J. Neurosurg 95. https://doi.org/10.3171/spi.2001.95.2.0208.
Wu, A., March, L., Zheng, X., Huang, J., Wang, X., Zhao, J., Blyth, F.M., Smith, E., Buchbinder, R., Hoy, D., 2020. Global low back pain prevalence and years lived with disability from 1990 to 2017: estimates from the Global Burden of Disease Study 2017. Ann. Transl. Med. 8. 10.21037/atm.2020.02.175.
Zhang, Z.-M., Zhao, L., Qu, D.-B., Jin, D.-D., 2009. Artificial nucleus replacement: surgical and clinical experience. 10.1111/j.1757-7861.2008.00010.x.
Zheng, C.J., Chen, J., 2015. Disc degeneration implies low back pain. Theor. Biol. Med. Model 12. https://doi.org/10.1186/s12976-015-0020-3.